

University of Groningen

## Electronic states and phases of KxC60 from photoemission and X-ray absorption spectroscopy

Chen, C.T.; Tjeng, L.H.; Rudolf, Petra; Meigs, G.; Rowe, J.E.; McCauley Jr, J.P.; Smith III, A.B.; McGhie, A.R.; Romanow, W.J.; Plummer, E.W.

*Published in:*  
Nature

*DOI:*  
[10.1038/352603a0](https://doi.org/10.1038/352603a0)

**IMPORTANT NOTE: You are advised to consult the publisher's version (publisher's PDF) if you wish to cite from it. Please check the document version below.**

*Document Version*  
Publisher's PDF, also known as Version of record

*Publication date:*  
1991

[Link to publication in University of Groningen/UMCG research database](#)

*Citation for published version (APA):*

Chen, C. T., Tjeng, L. H., Rudolf, P., Meigs, G., Rowe, J. E., McCauley Jr, J. P., ... Plummer, E. W. (1991). Electronic states and phases of KxC60 from photoemission and X-ray absorption spectroscopy. *Nature*, 352(6336). DOI: 10.1038/352603a0

### Copyright

Other than for strictly personal use, it is not permitted to download or to forward/distribute the text or part of it without the consent of the author(s) and/or copyright holder(s), unless the work is under an open content license (like Creative Commons).

### Take-down policy

If you believe that this document breaches copyright please contact us providing details, and we will remove access to the work immediately and investigate your claim.

*Downloaded from the University of Groningen/UMCG research database (Pure): <http://www.rug.nl/research/portal>. For technical reasons the number of authors shown on this cover page is limited to 10 maximum.*

power-law dependence on the current, particularly if multiple inelastic scattering events are required. The observed sideways motion of the xenon atom at greater tip-sample separation is consistent with the xenon atom being vibrationally excited. The absence of sideways motion at closer tip-sample separation may be due to the increased van der Waals attraction to the tip as the tip is brought closer to the surface. Heating-assisted electromigration is the only mechanism of which we are aware that is consistent with all the observed phenomena.

Note that the atom switches we have constructed are macroscopic devices in the sense that most of the power dissipation occurs not in the atomic-scale volume of the active element but in a volume comparable to the cube of the inelastic mean free path of electrons in the terminals of the switch. Furthermore, our macroscopic terminals do not show the quantum size effects that atomic-scale leads would exhibit.

It is clear that serious obstacles lie between what we have demonstrated and the realization of a genuinely useful atomic-scale device<sup>16</sup>. The prospect of atomic-scale logic and memory devices is nonetheless a little closer. We are intrigued by the idea that atom switches might already exist in the form of single cage-like molecules which derive their switching function from an atom that is trapped in the cage. □

Received 15 July; accepted 23 July 1991.

1. Hansma, P. K. & Tersoff, J. *J. appl. Phys.* **61**, R1-R23 (1987).
2. Lyo, I.-W. & Avouris, P. *Science* **245**, 1369-1371 (1989).
3. Bedrossian, P., Chen, D. M., Mortensen, K. & Golovchenko, J. A. *Nature* **342**, 258-260 (1989).
4. Eigler, D. M. & Schweizer, E. K. *Nature* **344**, 524-526 (1990).
5. *New Scientist* **129**, 20 (23 Feb. 1991).
6. *New Scientist* **26**, 31 (26 Jan. 1991).
7. Becker, R. S., Golovchenko, J. A. & Swartzentruber, B. S. *Nature* **325**, 419-421 (1987).
8. Fuchs, H. & Schimmel, T. *Adv. Mater.* **3**, 112-113 (1991).
9. Mamin, H. J., Guethner, P. H. & Rugar, D. *Phys. Rev. Lett.* **65**, 2418-2421 (1990).
10. Whitman, L. J., Strosio, J. A., Dragoset, R. A. & Celotta, R. J. *Science* **251**, 1206-1210 (1991).
11. Lyo, I.-W. & Avouris, P. *Science* **253**, 173-176 (1991).
12. Haberland, H., Kolar, T. & Reiners, T. *Phys. Rev. Lett.* **63**, 1219-1222 (1989).
13. Eigler, D. M., Weiss, P. S., Schweizer, E. K. & Lang, N. D. *Phys. Rev. Lett.* **66**, 1189-1192 (1991).
14. Ralls, K. S., Ralph, D. C. & Buhrman, R. A. *Phys. Rev.* **B40**, 11561-11570 (1989).
15. Verbruggen, A. H. *IBM J. Res. Dev.* **32**, 93-98 (1988).
16. Landauer, R. *Physica A168*, 75-87 (1990).

ACKNOWLEDGEMENTS. We thank D. J. Auerbach for fostering an environment which stimulated this work. We are also grateful to H. Otto, R. B. Martin and J. Downey for their questions.

## Electronic states and phases of $K_xC_{60}$ from photoemission and X-ray absorption spectroscopy

C. T. Chen\*, L. H. Tjeng\*, P. Rudolf\*, G. Meigs\*,  
J. E. Rowe\*, J. Chen†, J. P. McCauley Jr†,  
A. B. Smith III†, A. R. McGhie†, W. J. Romanow†  
& E. W. Plummer†

\* AT&T Bell Laboratories, Murray Hill, New Jersey 07974, USA

† Laboratory for Research on the Structure of Matter, University of Pennsylvania, Philadelphia, Pennsylvania 19104, USA

HIGH-resolution photoemission and soft X-ray absorption spectroscopies have provided valuable information on the electronic structure near the Fermi energy in the superconducting copper oxide compounds<sup>1-4</sup>, helping to constrain the possible mechanisms of superconductivity. Here we describe the application of these techniques to  $K_xC_{60}$ , found recently to be superconducting below 19.3 K for  $x \approx 3$  (refs 5-7). The photoemission and absorption spectra as a function of  $x$  can be fitted by a linear combination of data from just three phases,  $C_{60}$ ,  $K_3C_{60}$  and  $K_6C_{60}$ , indicating that there is phase separation in our samples. The photoemission spectra clearly show a well defined Fermi edge in the  $K_3C_{60}$  phase with a density of states of  $5.2 \times 10^{-3}$  electrons  $eV^{-1} \text{ \AA}^{-3}$  and an occupied-band width of 1.2 eV, suggesting that this phase may be

a weakly coupled BCS-like (conventional) superconductor. The  $C_{1s}$  absorption spectra show large non-rigid-band shifts between the three phases with half and complete filling, in the  $K_3C_{60}$  and  $K_6C_{60}$  phases respectively, of the conduction band formed from the lowest unoccupied molecular orbital of  $C_{60}$ . These observations clearly demonstrate that the conduction band has  $C_{2p}$  character. The non-rigid-band shift coupled with the anomalous occupied-band width implies that there is significant mixing of the electronic states of K and  $C_{60}$  in the superconducting phase.

A mixture of fullerenes was synthesized by contact arc evaporation<sup>8</sup> of graphite under 300 torr of He. After Soxhlet extraction with toluene,  $C_{60}$  was separated from the mixture by column chromatography on neutral alumina with 5% toluene in hexane as eluant. The purity of  $C_{60}$  was >99.9% relative to  $C_{70}$  impurity. The sample was bulk-dried under vacuum for several hours at 200 °C, then heated in flowing  $N_2$  to 325 °C before use. Pure  $C_{60}$  (ref. 8) was evaporated from a pyrex ampule in an ultrahigh-vacuum chamber and potassium was obtained from a SAES getter source. Both sources were outgassed for several hours after the system was baked.  $C_{60}$  was deposited onto a clean Cu(100) substrate at room temperature until a film of thickness  $\geq 200 \text{ \AA}$  was obtained. Potassium was evaporated onto the carbon film which was subsequently annealed at 100 °C for  $\sim 1$  h. After the sample had returned to room temperature, the photoemission and absorption spectra were recorded. The concentration of potassium was controlled by sequential evaporation and annealing steps until a saturated  $K_6C_{60}$  sample was obtained. All spectra were measured using the AT&T Bell Laboratories Dragon high-resolution soft X-ray beam line at the National Synchrotron Line Source<sup>9,10</sup>, with the experimental resolution set at 120 meV for photoemission spectra, 60 meV for absorption spectra.

Figure 1 shows a set of photoemission spectra of the valence-band region of  $K_xC_{60}$  as a function of the K concentration. The bottom curve is for pure  $C_{60}$ , which is nearly identical to the spectrum published by Weaver *et al.*<sup>11</sup>. The second curve labelled  $\bar{x} = 0.5$  has basically the same features as the pure  $C_{60}$  spectrum, except that the small concentration of K has created a Fermi edge 2.6 eV above the highest occupied molecular orbital (HOMO) peak of  $C_{60}$ . As the K concentration is increased by sequential evaporation and annealing, the valence-band spectra can be seen to change. The most marked change is the clear

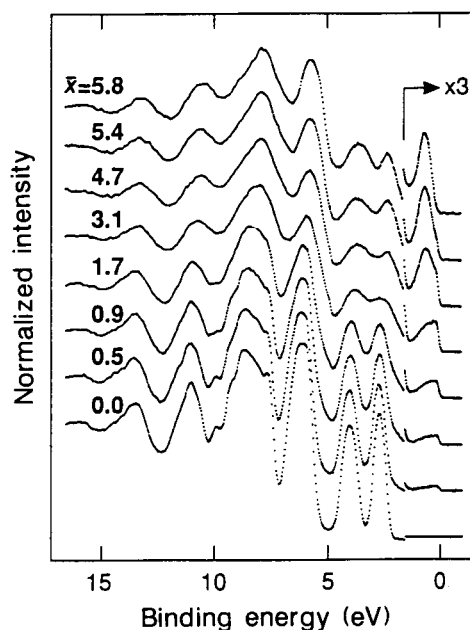


FIG. 1 Valence-band photoemission spectra of  $K_xC_{60}$  as a function of  $x$ . The Fermi edge region has been enlarged ( $\times 3$ ) with the background subtracted. Energy  $h\nu = 110$  eV.

development of a Fermi edge; that is, the sample becomes metallic. The region near the Fermi energy ( $\epsilon_F$ ) shows that the sample starts as an insulator, becomes a metal with a maximum density of states (DOS) at  $\epsilon_F$  for  $x=3$ , and is nonmetallic at  $x=6$ . This is consistent with theoretical calculations for both  $C_{60}$  (refs 11, 12) and  $K_6C_{60}$  (ref. 13), as well as with the conductivity measurements on  $K_xC_{60}$  (ref. 14).

Figure 2 shows the soft X-ray absorption spectra for the same sequence of K concentrations depicted in the valence-band spectra of Fig. 1. The lowest-energy peak in the spectrum for  $C_{60}$  is the transition from the C 1s to the lowest unoccupied molecular orbital (LUMO). There are significant changes in the soft X-ray absorption spectra as the K concentration increases; the intensity of the excitation to the LUMO of  $C_{60}$  decreases while the intensity of the K  $2p \rightarrow 3d$  absorption (near  $h\nu = 297$  eV) increases.

Two previous reports of the photoemission spectra of  $K_xC_{60}$  have been published<sup>15,16</sup>, but neither of these investigations shows the clear development of the Fermi level intensity as seen in Fig. 1. No soft X-ray absorption spectra have been reported for  $K_xC_{60}$ .

The K concentration was determined in three ways: using the intensity of the peak near  $\epsilon_F$  in Fig. 1, the intensity of the K absorption in Fig. 2 and a fitting procedure applied to the absorption spectra, described later. The average concentration  $\bar{x}$  is shown in the figures. The sampling depth in these three measurements is somewhat different, producing slight variations (of the order of  $\pm 10\%$ ) in the measured concentration.

The data presented in Fig. 1 for the valence-band structure near  $\epsilon_F$  indicate that there are only three phases:  $C_{60}$  with no structure within  $\sim 2$  eV of  $\epsilon_F$ ,  $K_3C_{60}$  with a conduction band crossing  $\epsilon_F$  and  $K_6C_{60}$  with a filled band  $\sim 0.6$  eV below  $\epsilon_F$ . Figure 3 shows this region of the spectra for these three phases. The curve for  $K_3C_{60}$  was generated from the  $\bar{x}=3.1$  curve by removing a small contribution from the saturated spectrum. The DOS at  $\epsilon_F$  can be directly measured from the spectral intensity at  $\epsilon_F$  after the instrumental broadening has been removed. The conversion of the intensity scale to states per electron volt per  $C_{60}$  molecule is accomplished by using the HOMO of the  $K_6C_{60}$  as a reference. This band is derived from the LUMO of  $C_{60}$  which contains three states (six electrons). An alternative normalization using the area of the conduction band itself gives almost identical results. Our measured DOS at  $\epsilon_F$  is  $1.9 \pm 0.1$  states per eV per  $K_3C_{60}$ , equivalent to  $5.2 \times 10^{-3}$  electrons  $eV^{-1} \text{ \AA}^{-3}$ . To extract the occupied-band width of the conduction

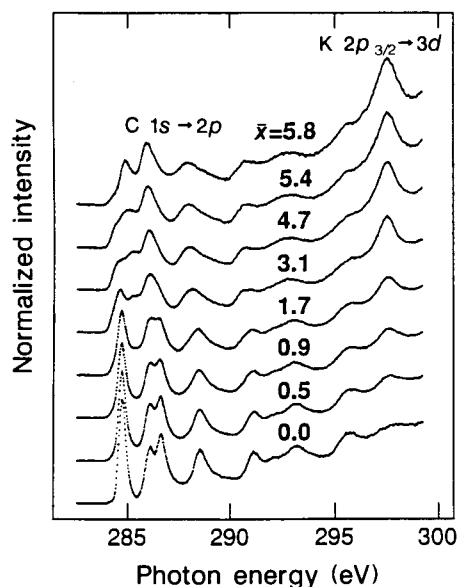


FIG. 2 Soft X-ray absorption spectra of  $K_xC_{60}$  as a function of  $x$ .

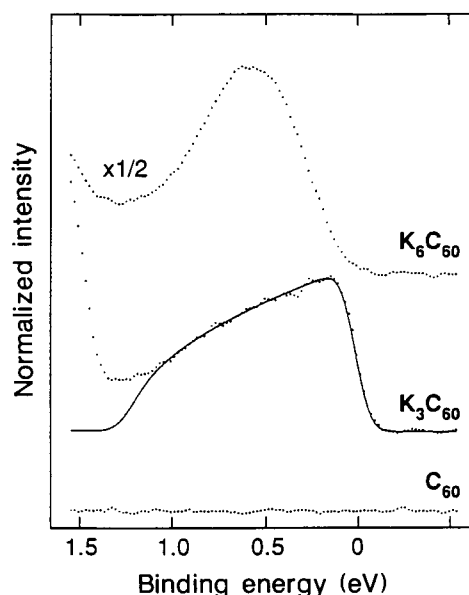


FIG. 3 Photoemission spectra near the Fermi edge for three phases of  $K_xC_{60}$  ( $h\nu=110$  eV).

band of  $K_3C_{60}$ , the data are fitted with a free-electron-like (FE) band,  $N(\epsilon) = N(\epsilon_F) [(\epsilon - \epsilon_0)/(\epsilon_F - \epsilon_0)]^{1/2}$ , convoluted with a gaussian instrumental response function (solid line). The occupied-band width is found to be  $1.2 \pm 0.05$  eV. As this band is derived from the C  $2p$  atomic orbitals, a tight-binding-like (TB) band has also been used to fit the data. The standard deviation of the TB fit (not shown) is two times larger than that of the FE fit, but gives a similar occupied-band width. This occupied-band width in  $K_3C_{60}$  is almost the same as the full-band width of the HOMO in  $K_6C_{60}$ . In weak-coupling BCS theory, the transition temperature is related to the DOS by the relationship  $kT_c = 1.13E \exp[-1/(N(\epsilon_F)V_0)]$ , where  $E$  is the energy of the pairing-mediation excitation,  $V_0$  is the electron-excitation coupling strength and  $\lambda = NV_0$  is the coupling constant. Cheng and Klein<sup>17</sup> have calculated the phonon modes for both the face-centred cubic and body-centred cubic phases of  $K_3C_{60}$ , observing that the low-energy translational and librational motions of the  $C_{60}$  molecules are strongly coupled to the K motion. If we use the energy of  $30 \text{ cm}^{-1}$  found for the face-centred cubic phase, we obtain a value of  $\lambda = 1.06$ , which is large for weak coupling. This value of  $\lambda$  is then due to the low frequency of the coupled librational-translational modes and should be considered as an upper limit. Even for this  $\lambda$  we have  $V_0 = 0.56$  eV, corresponding to a deformation potential  $\partial V/\partial u = 0.27 \text{ eV \AA}^{-1}$ . This is a relatively modest matrix element for electron-phonon scattering, consistent with  $K_3C_{60}$  being a BCS superconductor.

The original X-ray diffraction studies of  $K_xC_{60}$  powders indicated that for  $0 < x < 6$  the sample was almost completely phase-separated into  $C_{60}$  and  $K_6C_{60}$  (ref. 18), consistent with the first report of superconductivity in  $K_3C_{60}$ , where it was claimed that only 1% of the sample contributed to the superconducting phase<sup>5</sup>. Recently, Holczer *et al.*<sup>7</sup> showed that there was a single superconducting phase  $K_3C_{60}$ , which is now believed to be face-centred cubic with K incorporated into all of the octahedral and tetrahedral interstices<sup>19</sup>. All of the spectral features near  $\epsilon_F$  in Fig. 1 can be fitted with the three pure-phase spectra shown in Fig. 3. It is slightly more difficult to fit the absorption spectra in a similar fashion, because the three phases have markedly different structures. The absorption spectrum for pure  $K_3C_{60}$  was constructed from the difference between the spectrum for  $\bar{x}=0.9$  and the pure  $C_{60}$  spectrum and from the difference between the last two curves in the doping sequence. The assumption was that if there is phase separation, as indicated by the

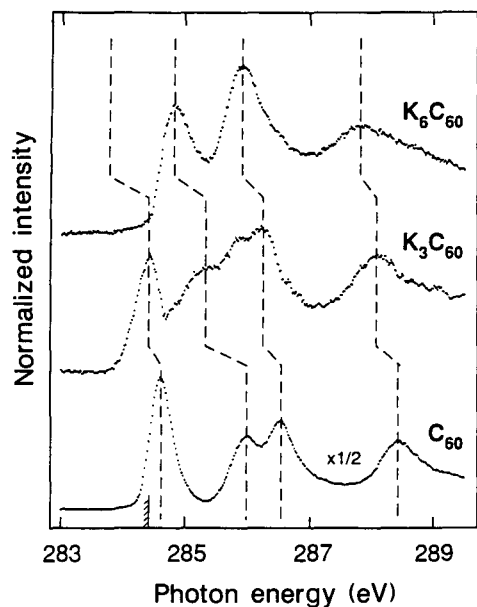


FIG. 4 C 1s absorption spectra for the three phases of  $K_xC_{60}$ . The shaded vertical line at the bottom indicates the C 1s excitation threshold for the superconducting phase.

valence photoemission curves, then this procedure should give the same spectrum for  $K_3C_{60}$  in the limits of low and high K concentration. This assumption is justified by internal consistency tests of the absorption data, where all spectra can be fitted by combinations of the three pure-phase spectra,  $C_{60}$ ,  $K_3C_{60}$ , and  $K_6C_{60}$ , shown in Fig. 4.

The width of the peak in the  $K_3C_{60}$  absorption spectrum at the threshold is due almost entirely to the width of the carbon core level. This sharp peak indicates that there is an edge singularity effect in the excitation spectrum from  $K_3C_{60}$ , that is, a metallic exciton. Energy bands of similar character are found to shift toward the excitation threshold in the three phases. The area of the threshold peak in the  $K_3C_{60}$  spectrum is exactly half the area of the LUMO in  $C_{60}$ . The important observation is that there is not a rigid-band shift of the  $C_{60}$  orbitals in these three phases. These observations clearly demonstrate the C 2p character of the energy band near  $\epsilon_F$  observed in photoemission. Coupled with the anomalous occupied-band width in  $K_3C_{60}$ , these results imply a considerable hybridization between the electronic states of K and  $C_{60}$  in the superconducting phase. Presumably, this hybridization is responsible for the electron-phonon coupling, which together with the relatively high value of the DOS at  $\epsilon_F$  suggests that  $K_3C_{60}$  may be a weak-coupling BCS-type superconductor. □

## Magnetic-field penetration depth in $K_3C_{60}$ measured by muon spin relaxation

Y. J. Uemura\*, A. Keren\*, L. P. Le\*, G. M. Luke\*, B. J. Sternlieb\*, W. D. Wu\*, J. H. Brewer†, R. L. Whetten‡, S. M. Huang‡, Sophia Lin‡, R. B. Kaner‡, F. Diederich‡, S. Donovan§, G. Grüner§ & K. Holczer§

\* Department of Physics, Columbia University, New York, New York 10027, USA

† TRIUMF and Department of Physics, University of British Columbia, Vancouver, British Columbia, V6T 2A3, Canada

‡ Department of Chemistry and Biochemistry, University of California, Los Angeles, California 90024, USA

§ Department of Physics, University of California, Los Angeles, California 90024, USA

THE discovery<sup>1-3</sup> of superconductivity in  $C_{60}$  doped with the alkali metals potassium and rubidium has introduced a new family of three-dimensional molecular superconductors<sup>4</sup>. The potassium-doped compound<sup>3</sup>  $K_3C_{60}$  has a relatively high transition temperature ( $T_c = 19.3$  K), a very high upper critical field ( $H_{c2}(T \rightarrow 0) \approx 50$  T) and a short superconducting coherence length<sup>5</sup> ( $\xi = 26$  Å), in common with the copper oxide superconductors. Here we report muon-spin-relaxation measurements of the magnetic-field penetration depth  $\lambda$  in  $K_3C_{60}$ . The temperature dependence of  $\lambda$  and of the muon spin relaxation rate indicate that the superconducting energy gap is isotropic, without nodes or zero points. The low-temperature penetration depth  $\lambda(T \rightarrow 0)$  is about 4,800 Å, which implies a ratio of superconducting carrier density to effective mass to be  $n_s/(m^*/m_e) = 1.2 \times 10^{20} \text{ cm}^{-3}$  if one assumes the 'clean limit'. Combining this result with the value of  $\xi$ , we estimate the Fermi temperature  $T_F = 470$  K. In the relationship between  $T_F$  and  $T_c$ ,  $K_3C_{60}$  conforms to the trend exhibited by 'exotic' superconductors<sup>6,7</sup> such as the Chevrel phase compounds, the copper oxides and the organic BEDT systems.

The muon-spin-relaxation ( $\mu$ SR) technique has been extensively applied in the study of the penetration depth in various type-II superconductors<sup>8-10</sup>. In transverse-field  $\mu$ SR (TF- $\mu$ SR) measurements of  $\lambda$ , we apply an external magnetic field  $H_{ext}$  ( $H_{c1} \ll H_{ext} \ll H_{c2}$ ), and observe the spin precession of positive muons implanted in the specimen. In the superconducting state, the field  $H_{ext}$  forms a lattice of flux vortices in the specimen, resulting in a local magnetic field  $B$  having a distribution with a width  $\Delta B$  proportional to  $\lambda^{-2}$ . In the spectra of muon spin precession, the oscillation amplitudes are damped because of the inhomogeneity of the local field  $B$ . This damping is usually described by a gaussian envelope  $G_x(t) = \exp(-\frac{1}{2}\sigma^2 t^2)$  which defines the muon spin relaxation rate  $\sigma \propto \Delta B \propto \lambda^{-2}$ .

The specimen of  $K_3C_{60}$  was prepared at UCLA following the procedures described in ref. 3. A polycrystalline powder material weighing 135 mg was pressed into a sintered pellet  $\sim 1$  cm in diameter and 1 mm thick. Before pressing, the powder sample showed a shielding diamagnetism ranging from 40 to 60% of a bulk niobium reference. The difference from the reference is mostly due to the small packing density of the powder. Pressing and sintering results in an onset of bulk (100%) shielding at a temperature  $\sim 1$  K lower than  $T_c = 19.3$  K (ref. 11). X-ray studies on a similar specimen<sup>4</sup>, sensitive to microscopic-scale inhomogeneity, set an upper limit of 15% volume fraction for presumably nonsuperconducting minority phases. The sintered specimen for  $\mu$ SR was mounted in a  $^4\text{He}$  gas flow cryostat with its face normal to the beam direction along which the external field was applied. During the whole procedure of sample preparation and  $\mu$ SR measurements, the specimen was kept under vacuum or in dry He gas, except for an interval of less than 1

Received 26 June; accepted 26 July 1991.

1. Fujiwara, A., Takayama-Muromachi, E., Uchida, Y. & Okai, B. *Phys. Rev.* **B35**, 8814 (1987).
2. van der Marel, D., van Elp, J., Sawatzky, G. A. & Heitmann, D. *Phys. Rev.* **B37**, 5136 (1988).
3. Shen, Z.-X. *et al. Phys. Rev.* **B36**, 8414 (1987).
4. Chen, C. T. *et al. Phys. Rev. Lett.* **66**, 104 (1991).
5. Hebard, A. F. *et al. Nature* **350**, 600-601 (1991).
6. Rosseinsky, M. J. *et al. Phys. Rev. Lett.* **66**, 2830-2832 (1991).
7. Holczer, K. *et al. Science* **252**, 1154-1157 (1991).
8. Krätschmer, W., Lamb, L. D., Fostropoulos, K. & Huffman, D. R. *Nature* **347**, 354-358 (1990).
9. Chen, C. T. *Nucl. Instr. Methods* **A256**, 595 (1987).
10. Chen, C. T. & Settle, F. *Rev. Sci. Instrum.* **60**, 1616-1621 (1989).
11. Weaver, J. H. *et al. Phys. Rev. Lett.* **66**, 1741-1744 (1991).
12. Martins, J. L., Troullier, N. & Weaver, J. H. *Chem. Phys. Lett.* **180**, 457-460 (1991).
13. Erwin, S. C. & Pederson, M. R. *Phys. Rev. Lett.* (submitted).
14. Haddon, R. C. *et al. Nature* **350**, 320-322 (1991).
15. Benning, P. J., Martins, J. L., Weaver, J. H., Chibante, L. P. F. & Smalley, R. E. *Science* **252**, 1417-1419 (1991).
16. Wertheim, G. K. *et al. Science* **252**, 1419-1521 (1991).
17. Cheng, A. & Klein, M. L. *Phys. Rev. Lett.* (submitted).
18. Zhou, O. *et al. Nature* **351**, 462-464 (1991).
19. Stephens, P. W. *et al. Nature* **351**, 632-634 (1991).

ACKNOWLEDGEMENTS. We thank E. J. Mele, G. K. Wertheim and J. Zaanen for discussions. This research was partially funded by NSF. The National Synchrotron Light Source is supported by the DOE.